HEAT TRANSFER IN A 180DEG TURN RIBBED SQUARE CHANNEL

G. Cardone, T.Astarita and G. M. Carlomagno
DETEC - University of Naples

Keywords: *Rib, 180 deg turn, Heat transfer, Infrared Thermography*

Abstract

Local measurements of the heat transfer distribution nearby a 180deg sharp turn in a square channel with rib turbulators are carried out by means of infrared (IR) thermography associated to the heated-thin-foil technique. Ribs are mounted on two opposite walls and are placed at 30° with respect to the channel axis. Two rib pitches are used during the tests.

The convective heat transfer coefficient is evaluated from the measured temperature maps and the local bulk temperature of the flow which is obtained by making a one-dimensional energy balance along the channel. Results are presented in terms of local Nusselt number which is normalised with the classical Dittus and Boelter correlation. The fluid used during the test is air and the Reynolds number, based on the flow average velocity and channel hydraulic diameter, is 30,000.

1 Introduction

It is well known that in order to increase the thermodynamic efficiency of gas turbine engines is necessary to increase the gas entry temperature. Present advanced gas turbines operate at gas entry temperatures much higher than metal creeping temperatures and therefore require intensive cooling of their blades especially in the early stages.

A classical way to cool turbine blades is by internal forced convection: generally, the cooling air from the compressor is supplied through the hub section into the blade interior and, after flowing through a serpentine passage, is discharged at the blade trailing edge. The serpentine passage is mostly made of several adjacent straight ducts, spanwise aligned, which are connected by 180deg turns. The presence of these turns may cause modifications of the flow pattern with consequent high variations of the convective heat transfer coefficient.

Furthermore the presence of rib turbulators may completely change the flow field and hence the distribution of the local convective heat transfer coefficient. To increase the blade life, which depends both on its temperature and on the setting up thermal stresses, it is necessary to know the detailed distribution of the local convective heat transfer coefficient.

Due to the presence of a single rib, the main stream first separates, because of a recirculation zone ahead of it, and then reattaches, by creating a second recirculation zone behind the rib. If the ribs pitch is sufficiently larger than the rib height, which is the most practical case, the just described main flow features do not change if two or more ribs exist. The ribs presence increases the overall convective heat transfer coefficient both for the increased turbulent level and for the effects due to the reattachment.

Moreover, the angle that ribs make with the main stream induces a secondary flow that increases the convective heat transfer coefficient toward the upstream rib part with respect to the downstream one.

The effects of rib turbulators have been investigated by many researchers; in particular the works of Zhao and Tao [1], Ekkad and Han [2], Ekkad et al. [3], Park et al. [4], Akella and Han [5], Arts et al. [6] are acknowledged.

The main objective of this work is to produce, by means of infrared thermography, detailed and reliable local heat transfer

distributions in a ribbed channel with a 180° sharp turn. The requirement to produce such data is not only important *per se* but is also relevant to validate computer programs which are often used to study these complex flows. The use of infrared thermography in these types of problems may be advantageous because of its relatively good spatial resolution and thermal sensitivity. Moreover, the use of thermography satisfies both qualitative and quantitative requirements. The main features of this methodology are [7]: it is non-intrusive; it allows a complete two-dimensional mapping of the surface to be tested; digital image processing may be used to treat the infrared camera output.

2 Experimental Apparatus

Two symmetrical panels, shown in the sketch of Fig. 1, which consist of two adjacent straight ducts connected by a 180deg turn, are mounted together in order to form the test channel. Air from the ambient passes through the test channel, an orifice flow meter and is then aspirated from a centrifugal blower. The angular speed of the centrifugal blower (i.e. the mass flow rate) may be varied in a continuos way by means of an inverter. At the channel entrance, a honey-comb filter is mounted so as to reduce the ambient air turbulence and the *vena contracta* effect. The channel cross section, see Fig. 2, is 80*mm* wide and 80*mm* high. The 2000*mm* length ahead of the 180deg turn provides an almost hydro-dynamically fully developed flow before the turn. Tolerances are

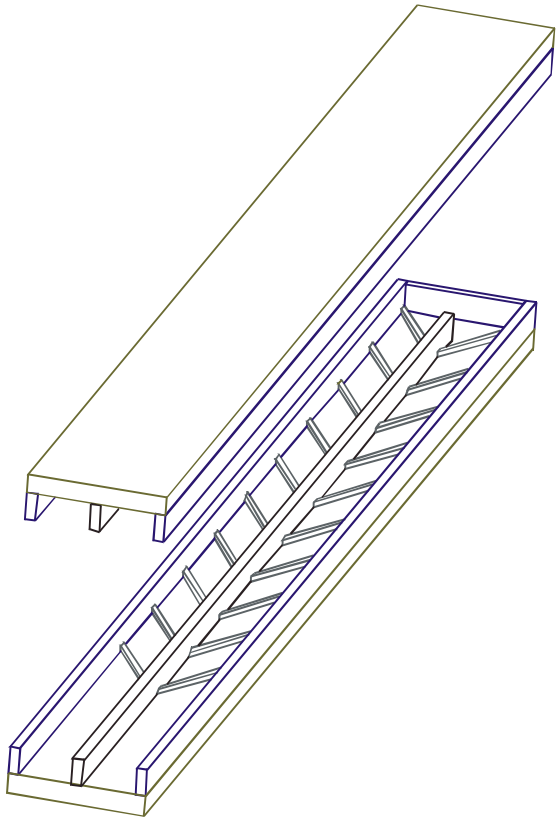

Fig. 1 – 3D Sketch of the test channel.

$\pm 0.5mm$ on channel width and $\pm 0.2mm$ on channel height. The central partition wall, which divides the two adjacent ducts, is 16*mm* thick.

The channel end lateral and partition walls are manufactured from 16x40*mm* fibreglass rectangular tubes, filled with polystyrene (so to have a low thermal conductance), which are mounted on two soft wood planks to constitute a panel. The coupling of the two panels generates

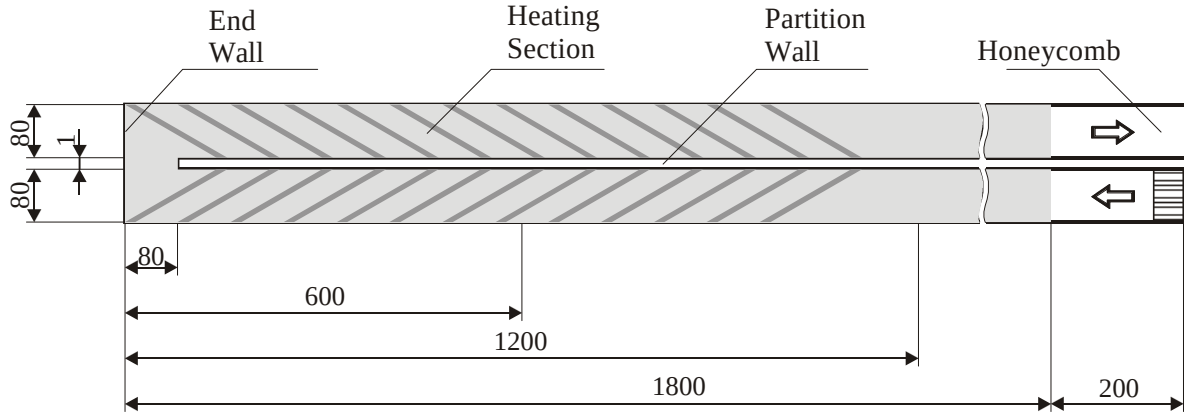

Fig. 2 – Test channel Plant.

the test channel. Between the lateral walls and each plank, for a length of about 1800*mm* towards the turn zone three printed circuit boards (600*mm* long each and connected in series) are placed. It is therefore possible to have two different heating boundary conditions, in particular: heating from one side (asymmetrical), or from two sides (symmetrical). The printed circuits are designed so as to achieve a constant heat flux over the channel surface (except beneath the lateral and partition walls) by Joule effect. Their tracks are 5*mm* thick, 1.8*mm* wide and placed at 2*mm* pitches; the overall thickness of each board is 0.53*mm*.

Square ribs (8*mm* high, so as to have a ratio between the channel and rib height of 10), made of aluminium (in order to have a high thermal conductance) are glued to the printed circuit boards and are placed at 30° with respect to the channel axis. Test are performed only on two symmetric configurations, which means that ribs on the lower and upper panels are facing each other. In the first configuration, which is shown in Fig. 2, the pitch between two successive ribs P is 80*mm*, giving a ratio between pitch and rib height e equal to 10 while, for the second one $P/e = 20$.

A stabilised DC power source supplies the electric current to the circuits and the power input is monitored by precisely measuring voltage drop and current across them. Two Pt100 RTD's measure the temperature at the entrance T_1 and at the outlet T_2 of the channel so as to monitor the overall increase of air temperature.

In the measurement zone (which goes up to 400*mm* from the end wall) one of the planks is cut so that the infrared camera has an optical access to the printed circuit board. Both the external (to channel) surface of the printed circuits boards (which is viewed by the infrared camera) and the internal one are coated with a thin layer of black paint which has emissivity coefficient equal to 0.95 in the wavelength of interest. The viewed surface is placed at the bottom of the channel (always heated) and is surrounded by black curtains so as to minimise both losses due to natural convection as well as unknown reflected radiation from the environment.

The infrared thermographic system employed is the AGEMA Thermovision 900. The field of view (which depends on the optics focal length and on the viewing distance) is scanned by the Hg-Cd-Te detector mainly in the 8-12*mm* infrared window. Nominal sensitivity, expressed in terms of noise equivalent temperature difference, is 0.07°C when the scanned object is at ambient temperature. The scanner spatial resolution is 230 instantaneous fields of view per line at 50% slit response function. A 10°x20° lens is used during the tests at a viewing distance of 1.1*m* which gives a field of view of about 0.24x0.48m^2 i.e. approximately one fourth of the heated zone; this is done so as to obtain a higher spatial resolution in the thermal image. Each image is digitised in a frame of 136 x 272 pixels at 12 bit. A dedicated software can perform on each thermal image: noise reduction by numerical filtering; computation of temperature and heat transfer correlations.

3 Data reduction

The infrared camera measures the temperature map of the external surface of the bottom wall which is correlated to the heat transfer coefficient by means of the steady state technique heated-thin-foil [7]. In particular, for each pixel of the digitised thermal image, the convective heat transfer coefficient h is computed as:

$$h = \frac{q_j - q_r - q_{nc} - q_k}{T_w - T_b} \qquad (1)$$

where: q_j is the uniform Joule heat flux, q_r the radiative flux to ambient and channel inside, q_{nc} the natural convection flux to ambient, q_k the conductive flux in the tangential (to wall) direction, T_w and T_b are the wall and the local bulk temperature, respectively. Because of the low value of the pertinent Biot number (which, in the worst case, is less than 0.01), the heated wall may be considered isotherm across its

thickness and therefore it is possible to measure the wall temperature at the outer side of the board.

The radiative thermal losses q_r are computed from the measured T_w and the ambient temperature by using the Stefan–Boltzmann law. To calculate losses due to natural convection some *ad hoc* tests are made in order to find an empirical correlation for the corresponding heat transfer coefficient. By applying this correlation, it is possible to estimate the thermal losses for natural convection with an error that is less of 15% of their value, introducing a total error in the evaluation of h lower than 0.3%.

A little more difficult is the procedure to compute the thermal losses due to tangential conduction. Details about this procedure are reported in [8].

The local bulk temperature T_b is evaluated by measuring the inlet temperature T_1 and by making a one-dimensional energy balance along the channel, i.e. along the channel main axis; triangular heating sections are considered in the turning zone. By measuring T_1, T_2 (the outlet temperature) and the air mass flow rate for each test run, an overall energy balance is also performed so as to compare the energy received by the fluid with the net electric power input. For all tests the maximum error found in this comparison is lower than 4%.

Heat transfer coefficients are computed in non-dimensional form by means of the local Nusselt number:

$$Nu = \frac{hD}{k} \qquad (2)$$

where D is the hydraulic diameter of the channel (which in the present case is 80.0mm) and k the thermal conductivity coefficient of air computed at film temperature (evaluated as $0.5(T_b + T_w)$ [9]).

Tests are carried out for Reynolds number Re equal to 30,000. Re is defined in the conventional way:

$$Re = \frac{VD}{n} \qquad (3)$$

where V and n are respectively the average velocity in the channel and the kinematic viscosity coefficient of air evaluated at average film temperature.

In order to compare the experimental results with those of literature, the Nusselt number is normalised by means of the classical Dittus and Boelter correlation for fully developed flow [10] as more recently interpreted by Kakac et al. [11]:

$$Nu^* = 0.024\, Re^{0.8}\, Pr^{0.4} \qquad (4)$$

4 Results and discussion

Experimental results are presented either in the form of visualisation of surface temperature, as well as local two-dimensional values of the normalised Nusselt number. In particular, herein, only results relative to Re = 30,000 and to a symmetrical heating boundary condition are reported.

When using an infrared scanning radiometer, one of the main advantages consists in the possibility to visualise the complete two-dimensional temperature distribution over the wall. Furthermore, if the sensor flux is based on the heated thin foil technique, by neglecting the heat losses q_r, q_{nc} and q_k, the temperature is inversely proportional to the convective heat transfer coefficient. In effect, also the continuous increase of the bulk temperature T_b along the channel (a few degrees Celsius) produces a slight modification of this behaviour.

The efficacy of thermography to perform this type of measurement is demonstrated by the thermograms of Fig. 3 which show the temperature maps of the channel heated wall for three ribs configuration and a Reynolds number practically equal to 30,000. As shown by the scale on the right side of the thermogram, each particular color represents a temperature band. Furthermore, it has to be stressed that temperature data in the neighbourhood of walls is not reliable since the latter, which are bonded to the printed circuit board and are not heated, tend to behave like fins in a stream and, therefore, produce a wall temperature decrease

a) Smooth channel;

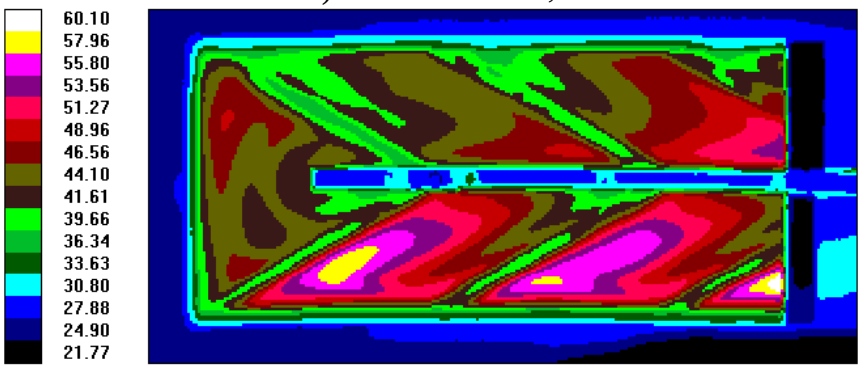

b) Ribbed channel (*P*/*e*=10);

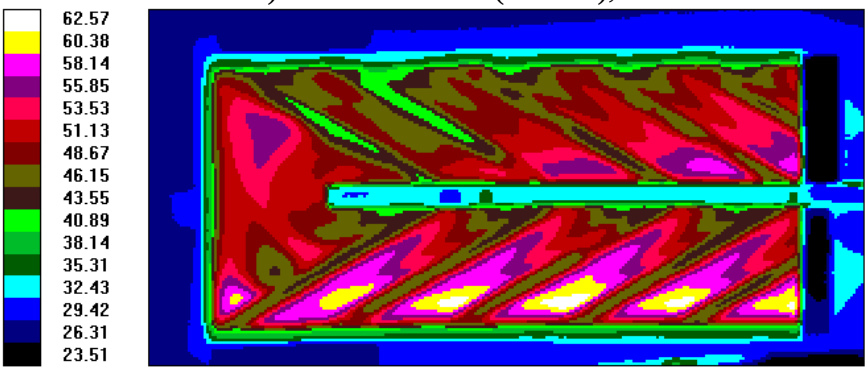

c) Ribbed channel (*P*/*e*=20);

Fig. 3 – Temperature maps (°*C*).

in their vicinity, owing to some thermal conduction within the board.

The first temperature map refers to the case of a smooth channel, i.e. a channel without ribs. By moving streamwise along the channel, the quasi-regular trend of the temperature distribution across the first duct (see Fig. 2), at the beginning of the measurement zone, proves a regular behaviour of the flow there. Three high heat transfer regions may be observed: the first one is placed nearby the end wall; the second one is located downstream of the second outer corner and extends for about 2 diameters; the third one is located 2 diameters after the second inner corner and is attached to the partition wall. These high heat transfer zones are due to the "jet" effect of the flow through the bend which has also been observed by previous authors [8]. In the figure it is also possible to see a low heat transfer zone in the first outer corner.

The other two temperature maps refer to the ribbed channels where the rib are clearly visible due to the higher heat transfer that occurs on them. Indeed the lower temperature, in the proximity of the rib, is mainly a consequence of the higher effective heat transfer

surface. The presence of the ribs completely alters the flowfield both in the straight channels and in the turning region. For both cases the flow is completely developed at the channel entrance and, in particular for P/e=10, the contours after the first and second rib are practically identical, the only differences due to some edge effects at the duct inlet.

The rib angle causes the formation of a secondary flow in the form of two counter rotating vortices. In the inlet channel, the main flow, in the proximity of both the bottom and

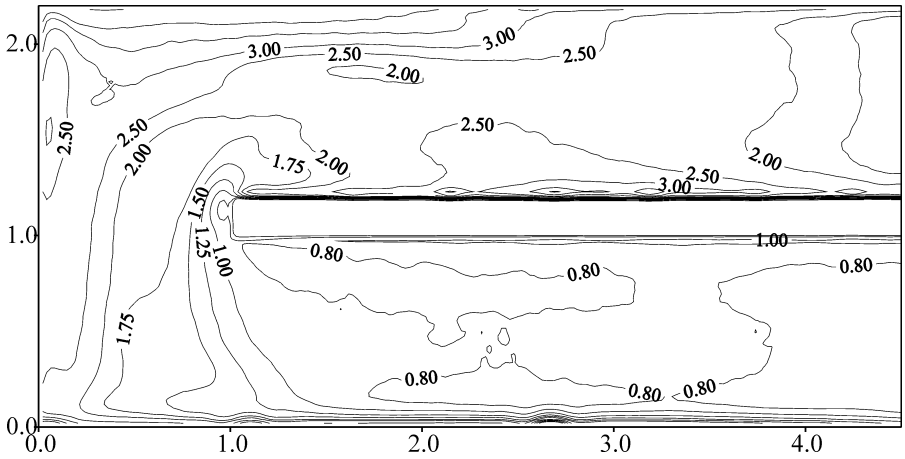

a) Smooth channel;

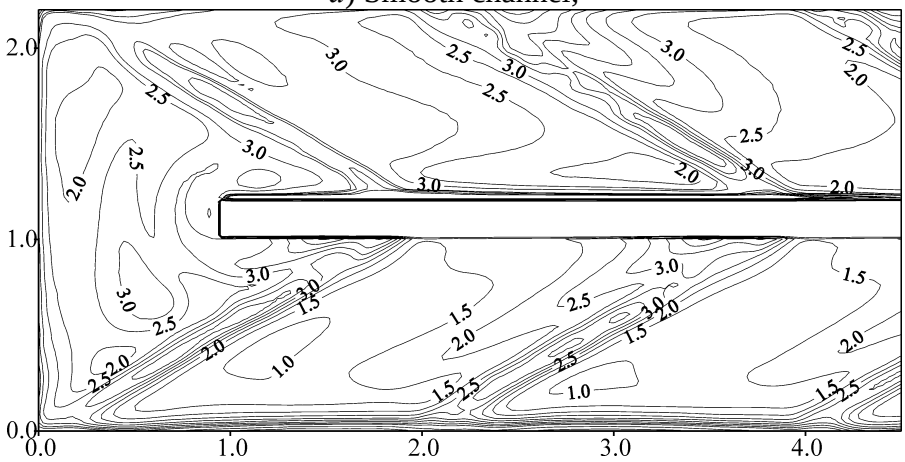

b) Ribbed channel (P/e=10);

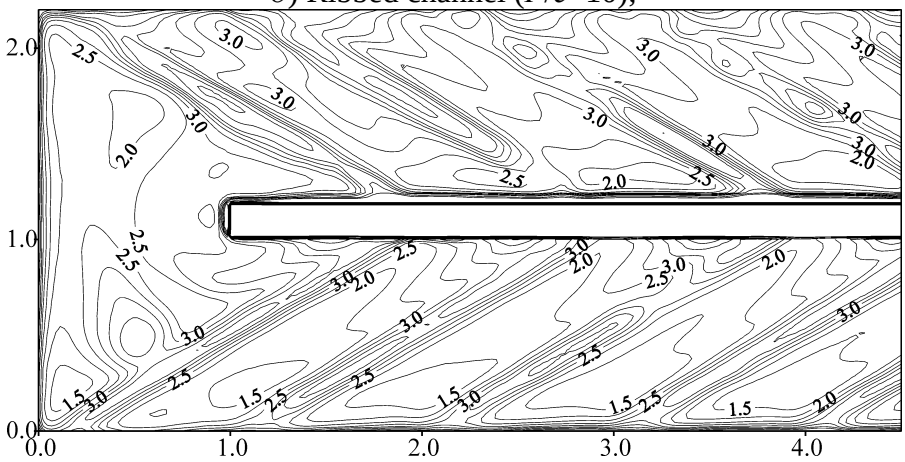

c) Ribbed channel (P/e=20);

Fig. 4 – Normalized Nusselt number distributions

top wall planks, is entrapped by the ribs and tends to accelerate toward the external wall. The secondary flow after having licked the external wall goes back to the partition wall and then creates a jet effect on the bottom and top wall planks near the partition wall. This explains the temperature maps asymmetry; the jet effect tends to increase the convective heat transfer coefficient near the partition wall with respect to that near the external wall. In the outlet channel, the secondary flow is reversed augmenting the convective heat transfer coefficient toward the external wall with respect to that near the partition wall.

In the turn zone the temperature maps for the ribbed channel show a completely different behaviour with respect to the smooth channel. This can also be better seen from the normalized Nusselt number distributions of Fig. 4 which are relative to the same testing conditions of the previous figure. For P/e=10 in proximity of the first external angle it is possible to see a low heat transfer zone, due to a recirculation bubble, as already observed for the smooth channel. The interaction between the secondary flow and the sharp turn produces, just after the last rib, two high heat transfer zones and, between them, a local minimum. A similar configuration it is found also for P/e=20 but the minor relative importance of the secondary flow reduces the differences. Another low heat transfer zone is also observed in the second part of the bend and just before the outlet channel first rib. For P/e=20 this zone is placed near the second external corner and for decreasing rib pitch tends to move towards the partition wall.

The reattachment line, downstream of the ribs, is clearly identified by the locus of the normalized Nusselt number local maxima and its distance from the (previous) rib increases for the higher rib pitch.

For both pitches the overall increase of the turbulence due to the bend induces higher values of the normalized Nusselt number in the outlet duct but the percentage increase is lower than that relative to a smooth channel because of the rib induced turbulence. This should decrease the thermal stresses in the turbine blade.

5 Conclusions

Local measurements of the heat transfer distribution nearby a 180deg sharp turn in a square channel with and without rib turbulators are carried out by means of infrared (IR) thermography associated to the heated-thin-foil technique. Ribs are symmetrically mounted on two opposite wall and are placed at 30° with respect to the channel axis. Two pitches between successive rib are used during the tests.

Experimental data shows that the presence of ribs completely modifies the convective heat transfer distribution both in the straight channels and in the turning zone. The secondary flows, induced by the inclined ribs, explain the asymmetry of the normalized Nusselt number distributions in the inlet and outlet channel. The reattachment line, downstream of the ribs, is clearly identified and its distance from the previous rib increases for the higher rib pitch.

For both the ribbed and smooth channel it is possible to see a low heat transfer zone, due to a recirculation bubble, in proximity of the first external angle. Furthermore, for the ribbed channel, the interaction between the secondary flow and the sharp turn produces, just after the last rib, two high heat transfer zones and a local minimum between them.

References

[1] Zhao C. Y. and Tao W. Q. Effect of rib angle orientation on local mass transfer distribution around sharp 180 deg turn with rib-turbulators mounted in entire two-pass channels. *Heat Mass Transfer*, Vol. 32, N. 5, pp. 325-332, 1997.

[2] Ekkad S V. and Han J. C. Detailed heat transfer distributions in two-pass square channels with rib turbulators. *Int. J. Heat Mass Transfer*, Vol. 40, N. 11, pp 2525-2537, 1997

[3] Ekkad S V., Huang Y., Han J. C. Detailed heat transfer distributions in two-pass square channels with rib turbulators and bleed holes. *Int. J. Heat Mass Transfer*, Vol. 41, N. 23, pp 3781-3791, 1998.

[4] Park C. W., Lau S. C. and Kukreja R. T. Heat/mass transfer in a rotating two-pass channel with transverse ribs. *J. Thermophys. Heat Transfer*, Vol. 12, N. 1, pp. 80-86, 1998.

[5] Akella K. V. and Han J. C. Impingement cooling in rotating two-pass rectangular channels with ribbed

walls. *J. Thermophys. Heat Transfer* , Vol. 13, N. 3, pp 364-371, 1999.

[6] Arts T., Rau G., Cakan M., Vialonga J., Fernandez D., Tarnowski F. and Laroche E. Experimental and numerical investigation on flow and heat transfer in large-scale, turbine cooling, representative, rib-roughened channels, *Journal of Power and Energy*, Vol. 211, pp. 263-271, 1997.

[7] Carlomagno G. M., de Luca L. Infrared Thermography in Heat Transfer, in *Handbook of Flow Visualization*, W.J. Yang ed., pp. 531-553 Hemisphere, 1989.

[8] Astarita T. and Cardone G. Thermofluidynamic Analysis of the Flow in a Sharp 180° Turn Channel, *Experimental Thermal Fluid Science*, Vol. 20, pp. 188-200, 2000.

[9] Kreith F., *Principles of Heat Transfer*, Intext Educational Publishers, New York., 1973.

[10] Dittus P. W. and Boelter L. M. K. Heat Transfer in Automobile Radiators of the Tubular Type, Univ. Calif. Pub. Eng., Vol. 2, N. 13, pp. 443–461, 1930 (reprinted in *Int. J. Comm. Heat and Mass Transfer*, Vol. 12, pp. 3-22, 1985.).

[11] Kakac S., Shah R. K. and Aung W., *Handbook of Single Phase Flow Convective Heat Transfer*, Wiley, New York, 1987.